Tightly Focusing Properties of Radially Polarized doughnut Gaussian Beam through a Uniaxial Birefringent Crystal

M.Lavanya[1], D.ThiruArul[2], K.B.Rajesh[3]

[1]*Department of Physics, PSGR Krishnammal College for Women, Coimbatore, TamilNadu, India, 641004*
[2,3]*Department of Physics, Chikkanna Govt Arts College, Tiruppur, TamilNadu, India, 641602*

Abstract-The properties of radially polarized doughnut shaped beam tightly focused through a uniaxial birefringent crystal system is studied numerically by the use of vectorial diffraction theory for small birefringence condition. It is observed that many novel focal patterns such as sub wavelength scale focal spot, focal hole and flattop profiled focal spot evolved considerably when properly choosing the doughnut angle (θ0) of incident Doughnut Gaussian (DG) beam .We also observed that axial shifting of generated focal patterns is possible with increasing the birefringence value [Δn] of the uniaxial crystal. We expect such a possibility of tuning and shifting the generated focal patterns finds possible applications in optical trapping and manipulating of particles and in material processing.

Keywords: Uniaxial birefringent crystal; Radially polarized laser; Doughnut Gaussian Beam, focal shift.

I. INTRODUCTION

Tight focusing of laser beam has been an academically interesting topic because of its wide potential applications in optical trapping, optical data storage, and high-resolution microscopy [1-6]. Recently, researches have increasingly focused on tight focusing of radially polarized beams [2,7,8]. A sub wavelength focal spot with long focal depth can be obtained using radially polarized beams [7-9]. Tightly focused radially polarized beams have been many possible applications, such as optical trapping [10,11] and High-resolution microscopy [12,13]. In many optical imaging systems focal shift can be used to adjust field distance without mechanical component change. In optical trapping system, focal shift accompanying with focal switch will be used to transporting the trapped particles. For certain geometric parameters of the beam, the focal shift occurs and can be adjusted by phase shift and polarized direction by inserting the phase filters, amplitude filters or 4 pi configuration in the pupil plane of the objective [14-21]. However, the presence of phase filters or amplitude filters makes some applications more difficult or even impossible. However it is reported that the performance of 4 pi microscopy is significantly affected by aberration[22.23] .On the other hand, optically uniaxial crystals are capable of shifting the focal structure without employing additional amplitude or phase filters [24-28]. The variation of birefringence produce the focal shift, because of the phase difference (ΔW) between the ordinary and extraordinary modes in the uniaxial birefringent crystal. The properties of light beams propagating in birefringent materials have attracted many researchers for years [25,29,30]. The transmission of 2D and 3D Gaussian beams in to a uniaxial crystal system was developed by Stamnes and Dhayalan et.al., [31,32].A. Ciattoni et.al., analyzed the propagation of cylindrically symmetrical fields such as radial and azimuthally polarized vortex beam in the uniaxial crystal system [33,34]. The propagation of various kinds of laser beams in uniaxial crystals has been reported [35-37]. Recently, a new kind of radially polarized beam called doughnut Gaussian (DG) beam is introduced in a high NA focusing system to produce sub wavelength focal spot, focal hole and multiple spots [38,39].In this paper, based on the theoretical model of Ref. [25,27] we extend the analysis of tight focusing properties of radially polarized doughnut shaped beams through a uniaxial birefringent crystal. It is shown that the intensity distribution of focal structure in the focal region can be tuned and shift along the longitudinal axis with increasing the birefringence value [Δn].

II.THEORY

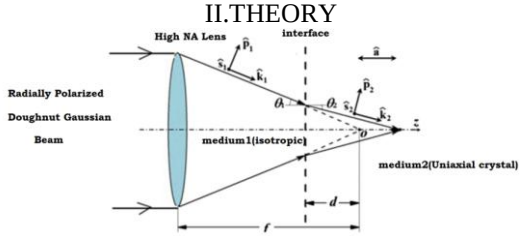

Fig 1: shows the schematic diagram of the focusing system

Here the radially polarized doughnut shaped beams is assumed to focus from medium 1 into medium 2 see Fig 1. Medium 1 is isotropic where as medium 2 is a uniaxial birefringent with its uniaxial symmetrical axis along optical axis. Here d is the probe depth which is the distance between the interface and geometrical focus. $\hat{k}_1$ And $\hat{k}_2$ are the wave vectors in medium 1 and medium 2 with $\hat{s}_1$ $\hat{p}_1$ and $\hat{s}_2$ $\hat{p}_2$ are the corresponding polarization vectors in parallel and perpendicular direction to the plane of incidence. Based on vectorial Debye theory [40], Cartesian components of the electric field vector in the focal region can be expressed as

$$E(\mathrm{r},\psi,\mathrm{z}) = \begin{bmatrix} E_x(\mathrm{r},\psi,\mathrm{z}) \\ \mathrm{E}_y(r,\psi,z) \\ E_z(r,\psi,z) \end{bmatrix} = E_x(r,\psi,z) = \frac{-iE_o}{\pi}\int_0^{\alpha}\int_0^{2\pi} \sin\theta_1\sqrt{\cos\theta_1}P(\theta_1,\phi)t_p \exp[ik_o(\mathrm{W}+\Delta\mathrm{W})]$$

$$\exp[ik_2 z\cos\theta_2 + ik_1 r\sin\theta_1\cos(\psi-\phi)]\begin{bmatrix}\cos\theta_2\cos\phi \\ \cos\theta_2\sin\phi \\ \sin\theta_2\end{bmatrix} d\phi d\theta_1 \quad (1)$$

Here E_o is a constant related to the focal length and the wavelength, $\alpha = \sin^{-1}(NA)$ is the maximal angle determined by the NA of the objective, t_p is the amplitude transmission coefficient for parallel polarization state which is given by the Fresnel equations [25]

$$t_p = \frac{2\sin\theta_2\cos\theta_1}{\sin(\theta_1+\theta_2)\cos(\theta_1-\theta_2)} \quad (2)$$

W_p = W + ΔW and W_s = W are the aberration functions of p- and s-polarizations respectively. Here W is the aberration function caused by the mismatch of the refractive indices medium 1 and medium 2,where ΔW is the phase difference between the ordinary and extraordinary modes in the uniaxial birefringent medium 2.W and ΔW are expressed as[25]

$$W = kd(n_2\cos\theta_2 - n_1\cos\theta_1), \Delta W = k(d+z)\Delta n\sin^2\theta_2/\cos\theta_2 \quad (3)$$

where k = 2π/λ is the wave number in vacuum and d is the distance between the interface and the geometric focus ;where Δn= $n_e - n_0$ represents the difference between the refractive indices of ordinary and extraordinary modes in the medium 2 which is the so-called birefringence (the ordinary and extraordinary refractive indices are n_0 and, n_e respectively, and $n_0 = n_2$).It is assumed that the focusing lens is corrected for aberrations introduced by anisotropic cover layer of thickness d and refractive index $n_2 = n_0$. As a result, $W_s = W = 0$, $W_p = \Delta W$.

Here $P(\theta_1,\phi) = \exp\left[-\left(\frac{\sin(\theta_1)-\theta_o}{\omega_o}\right)^2\right]$ is the pupil function of the incident doughnut Gaussian beam and is given by [38]. where ω_o reflects the beam size at the beam waist of the Gaussian beam. θ_o relates with the radius of the DG beam. Obviously, the shape of the defined doughnut Gaussian beam is determined by θ_o and ω_o. The focal properties are evaluated numerically for the incident radially polarized doughnut Gaussian beam by solving the above equations using the parameters NA = 0.95, n_1 = 1, n_2 = 1.5, λ = 632 nm, d = 150 μm.

III. RESULTS AND DISCUSSION

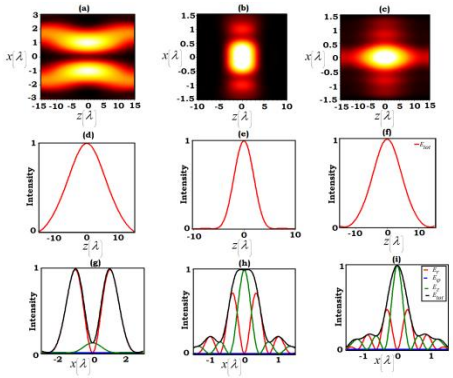

Fig (2): (a-c) are 3D Intensity distribution in the x-z plane corresponding to Δn=0 and for E_z =0.2, 0.84, 1.3. Fig (2): (d-f) are the corresponding axial intensity distribution. Fig (2): (g-i)are the intensity distribution in the transverse direction measured at the point of maximum axial intensity.

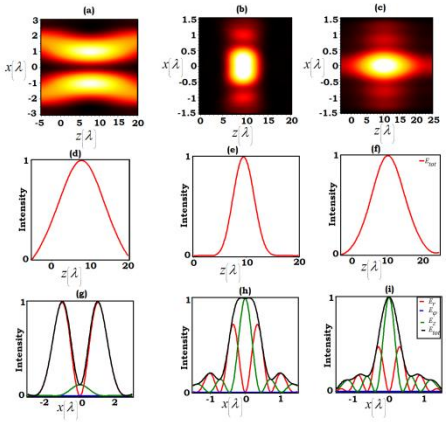

Fig (3): (a-c) are 3D Intensity distribution in the x-z plane corresponding to Δn=15 and for θ_o =0.2, 0.84, 1.3. Fig (3): (d-f) are the corresponding axial intensity distribution. Fig(3): (g-i)are the intensity distribution in the transverse direction measured at the point of maximum axial intensity.

Fig 2 and Fig 3 shows the focal structure obtained for incident radially polarized doughnut Gaussian beam with different doughnut angle θ_o in absence and presence of axial birefringence Δn . The position of the maximum field intensity depends on θ_o . For θ_o = 0, the beam governed by Eq. (1) is a conventional Gaussian beam. The width of the DG beam is determined by ω_o . In order to study the effect of the amplitude profile of the DG beam and those two parameters of the DG beam, here we fix the parameters NA =0.95 and ω_o=0.15 . Fig (2) shows the focal structure obtained for the DG beam with and for different θ_o in the absence of axial birefringence.It is noted from Fig 2 (a, d and g) when θ0 = 0.2, the generated focal structure is a focal hole having a slight residual intensity at the centre. The FWHM of the focal hole is noted as 0.90 λ where as its focal depth is 14.5 λ .It is noted from Fig 2 (g) the formation of focal hole is due to the domination of E_ϕ component having central minimum. However the residual intensity at the centre is due to the presence of weak longitudinal component E_z having central maximum. It is also noted from Fig 2 (b,e,h) that increasing θ_o=0.84, the generated focal segment is a flat topped profile having FWHM of 0.97 λ and focal depth of 4.49 λ . It is observed from Fig 2 (h) the formation of flat top profile is

due to the adjustment of E_r and E_z component in such a way the resultant focal structure is a flat-topped one in the radial axis. It is noted from Fig 2 (h) though the E_z component dominates the focal structure the proportion of the E_r component is such that the resultant total intensity structure is a flat-topped profile in radial axis. Fig 2 (c,f,i) shows that further increasing θ_o to 1.3 generated a sharp focal spot having FWHM of 0.67λ and focal depth of 12.3λ .From Fig 2 (i) it is noted that the formation of focal spot is due to the much dominating E_z component.
Fig 3 (a,d,i) shows the same as Fig 2 but for Δn=15. It is noted that the presence of axial birefringence shifted the maximum axial intensity of the generated focal hole to 7.5λ . It is noted that the FWHM of the generated focal hole is 0.90λ with focal depth of 14.5λ .Hence the presence of axial birefringence axially shifted the generated focal hole .Such a focal hole structure and its axial shifting is useful for trapping and manipulating particles of having refractive index lower than the ambient, cold atoms and in high resolution STED microscopy [21,41,42,43].Fig 3 (b,e,j) shows the presence of axial birefringence does not produce any structural change but it shifted the generated flat topped profile shape axially to a distance of 9.5λ from the geometrical plane. Such a flat top structure and axial shifting of the same is useful in tunable optical trapping, material processing, micro lithography, medical treatment [21,44-46]. Fig 3 (c,f,k) shows the presence of axial birefringence does not produce any structural change but it shifted the generated sharp focal spot from geometrical plane to 10.3λ . Such a sharp focal spot and its axial shifting having many applications [14,19,20,47-49].

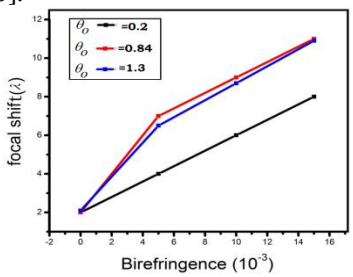

Fig 4: Dependence of the focal shift on the birefringence. The parameters for the calculation are the same as Fig. 2.

Fig 4 shows the relation between the focal shift and birefringence Δn. It can be seen that the focal shift increases with the increase of birefringence Δn and doughnut angle θ_o .The variation of birefringence has influence on the focal shift, because the phase difference ΔW between the ordinary and extraordinary modes in the uniaxial birefringent crystal.

Birefringence $\Delta n(10^{-3})$	Position of Maximum Intensity Shifted(λ)		
	Doughnut angle		
	$\theta_o = 0.20$ (focal hole)	$\theta_o = 0.84$ (flat top)	$\theta_o = 1.30$ (focal spot)
0	0	0	0
5	2.6	3.1	3.4
10	5.2	6.3	6.8
15	7.9	9.5	10.3

Table- 1. Showing the focal shift for different Δn and for θ_o

Table (1) shows the focal shift values for different birefringence value Δn and different doughnut angle θ_o

Hence the proposed system utilizing proper amplitude profile of incident beam and an uniaxial crystal system is much simpler and avoids the difficulties in fabricating and aligning various complex phase and amplitude filters and also the complicated 4 pi microscopic systems conventionally used to tune the focal patterns.

IV. CONCLUSION

In this article, the properties of tightly focused radially polarized doughnut Gaussian beam tightly focused through an uniaxial birefringent crystal is investigated numerically using vector diffraction theory. It is found from the numerical simulations, axial birefringence induce the focal shift along the longitudinal axis with increasing the

birefringence value [Δn]. In addition novel focal structures such as axially extended focal spot, focal hole, flattop profile can also obtained by changing the doughnut angle.

V.REFERENCE

[1] Zhang Z, Pu J, and Wang X, 2008 Opt. Lett. 33 49
[2] Youngworth K. S and Brown T. G 2000 Opt. Express 7 77
[3] Lerman G. M and Levy U 2007 Opt. Lett. 32 2194
[4] Walker P and Milster T. D 2001 Proc. SPIE 4443 73
[5] Helseth L. E 2002 Opt. Commun. 212 343
[6] Cheng, Gonçalves J. T, Golshani P, Arisaka K, and Portera-Cailliau C 2011 Nat. Methods 8 139
[7] Urbach H. P and Pereira S. F 2008 Phys. Rev. Lett. 100 123904
[8] Lin H, Jia B, and Gu M 2011 Opt. Lett. 36 2471
[9] Dorn R, Quabis S, and Leuchs G 2003 Phys. Rev. Lett. 91 233901
[10] Zhan Q 2004 Opt. Express 12 3377
[11] Zhang Y, Suyama T and Ding B 2010 Opt. Lett. 35 1281
[12] Sheppard C. J. R and Choudhury A 2004 Appl. Opt. 43 4322
[13] Zhan Q 2004 Opt. Express 12 3377
[14] Prabakaran K, Rajesh K.B, Pillai T.V.S, Chandrasekaran R, Jaroszewicz Z 2013 Opt Quant Electron 4 563-
[15] Li J, Gao X , Zhuang S, Huang 2010 Optik 121 821
[16] Gao P, Tian S, Weng X , Guo H 2016 J. Mod. Opt 1-6
[17] Yun M, Liang W, Kong W, Gao X, Zhu H, Liang 2010 J Opt. Commun.283 2079
[18] Gao X.M, Gao M.Y, Hu S, Guo H.M, Wang J, Zhuang S.L 2009 Nat. Science 1 229
[19] Yan S, Yao B, Rupp R 2011 Opt. Express 19 673
[20] Gao X, Hu S, Gu H, and Wang J 2009 Optik. 120 519
[21] Qiufang Zhan, Jinsong Li , Xiumin Gao 2009 Proc. of SPIE Vol. 7497 74970X-1
[22] Gould T.J, Burke D, Bewersdorf J, Booth M.J 2012 Opt. Express 20 20998
[23] Hao X, Antonello J, Allgeyer E. S., Bewersdorf J, Booth M. J 2017 Opt. Express 25 14049
[24] Wang S, Xie X, Gu M, Zhou J 2015 J. Opt. Soc. Am. A 32 1026
[25] Stallinga S 2001 J. Opt. Soc. Am. A. 18 2846
[26] Yonezawa K, Kozawa Y, Sato S 2008 J. Opt. Soc. Am. A 25 469
[27] Rao L.Z, Wang Z.C, Zheng X.X 2008 Chin. Phys. Lett. 25 3223
[28] Zhang Z, Pu J, Wang X 2008 Appl. Opt. 47 1963
[29] Fleck J. A, Jr. and Feit M. D 1983 J. Opt. Soc. Am. 73 920
[30] Ciattoni A , Ciattoni G and Palma C 2002 J. Opt. Soc. Am. A 19 792
[31] Stamnes J.J, Dhayalan V 2001 J. Opt. Soc. Am. A 18 1662
[32] Jain M, Lotsberg J.K, Stamnes J.J, Frette O, Velauthapillai D , Jiang D, Zhao X 2009 J. Opt. Soc. Am. A 26 691
[33] Ciattoni A, Cincotti G, Palma C 2002 J. Opt. Soc. Am. A 19 792
[34] Cincotti G, Ciattoni A, Sapia 2003 Opt. Commun. 220 33
[35] Deng D, Yu H, Xu S, Shao J and Fan Z 2008 281 202
[36] Zhou G, Chen R and Chu X 2012 Opt. Express 20 2196
[37] Deng D, Chen C, Zhao and Li H 2013 Appl. Phys. B 110 433
[38] Lin J, Chen R, Yu H, Jin P, Cada and Ma Y 2014 Opt. Laser Technol. 64 242
[39] Mohana Sundaram C, Prabakaran K, Rajesh K. B, Udhayakumar M, Anbarasan P. M, Mohamed Musthafa A 2016 Opt Quant Electron 48 507 1-12
[40] Gu M 2000 Advanced Optical Imaging Theory Berlin: Springer
[41] Gao X, Fei Z, Xu W and Gan F 2005 Optik. 116 99
[42] Xu P, He X.D, Wang J and Zhan M.S 2010 Opt. Lett. 35 2164
[43] Willig K.I, Rizzoli S. O, Westphal V, Jahn R and Hell S.W 2006 Nature 440 935
[44] Dickey F.M and Holswade S.C 2000 Laser Beam Shaping: Theory and Techniques Marcel Dekker
[45] Romero L.A, Dickey F.M 1996 J. Opt. Soc. Am. A 13 751
[46] Homburg O, Mitra T 2012 Proc. SPIE 8236 82360A
[47] Varin C, Piche and Porras M.A 2005 Phys. Rev. E 71 026603
[48] Dehez H, Piche M, De Koninck Y 2009 Opt. Lett. 34 3601
[49] Zhan Q 2004 Opt. Express 12 3377